Science of Sintering, **37** (2005) 77-92

UDK 621.927:622.785

Mechanism of Mechanochemical Synthesis of Complex Oxides and the Peculiarities of Their Nano-Structurization Determining Sintering

V.V. Zyryanov
Institute of Solid State Chemistry and Mechanochemistry SB RAS,
Novosibirsk, 630128 Kutateladze 18, Russia

Abstract:

A mechanism of superfast mechanosynthesis reaction for oxide systems is proposed on the base of a dynamics study. The threshold effect and linear dependence of the chemical response on the effective temperature of the reaction zone are established. Major factors are determined: molecular mass of reagents, enthalpy and difference of reagents in Mohs's hardness, which also influence the composition of the primary product. Primary acts are characterized by a superfast roller mechanism of mass transfer with the formation of a transient dynamic state (D). Secondary acts slowly approximate the composition of the product to the composition of the starting mixture by diffusion mass transfer in a deformation mixing regime with a contribution of a rotation (roller) mechanism. The list of structure types for complex oxides derived by mechanosynthesis includes perovskites, fluorites, pyrochlors, sheelites, and some other ones. Powders of crystal products display multilevel structurization. In all studied complex oxides strong disordering of the "anti-glass" type was observed. The mechanism of sintering was studied in $BaTiO_3$ powders of different origin and in metastable complex oxides derived by mechanosynthesis. The major contribution in shrinkage belongs to rearrangements of crystalline particles as a whole. Structure transformations accompany, as a rule, sintering of inhomogeneous powders derived by mechanosynthesis.*

Keywords: *Mechanosynthesis, nanopowders, complex oxides, disordering, sintering, ceramics.*

Introduction

Development of mechanochemistry as a powerful tool to modify a solid state and to obtain new defect states unachievable by other means is an important field and is stimulated mainly by modern materials science, needs of industry for new nano-materials and green technologies. The investigation goal of the mechanism of mechanosynthesis reactions is finding the major factors determining the dynamics of the process, as well as revelation of the possibilities of regulating the structure and properties of a product, that is, a traditional

*) Corresponding author: vladi@mail.nsk.ru

goal of solid state chemistry to adjust reactions in time and space. Compaction and sintering of oxide powders into dense ceramics finally determine the properties of materials, so understanding of physicochemical processes taking place during powder consolidation is also necessary for realization of the possibilities of the mechanochemical method. Because of this, the new approach to the development of materials was called mechanochemical ceramic method (MCM).

Mechanism of mechanosynthesis

Investigation of the mechanism of an unusual phenomenon, namely, superfast mechanochemical synthesis of mixed oxides with the melting points of reagents up to 3000 K at the room background temperature, is a solution to the problem of a double black box [1-2]. A complicated reaction of mechanosynthesis, accompanied by parallel processes, proceeds in devices with complicated multiple mechanical loading of the powders. The algorithm for solving this problem includes elimination of a device for energy supply to the powder (mechanical "black box") by creating identical conditions of mechanical treatment (MT), which is provided by the application of a correct procedure [3]. Such an approach provides the possibility to carry out a *relative* comparison of systems, which is sufficient to achieve the formulated goal, and to estimate mechanical energy supplied to the substance through a definite number of so-called averaged shocks. Along with macro-homogeneity and sharp decrease in contamination, a correct treatment procedure also provides approximately constant hollowness of the powder during MT, which gives a linear relation between time of MT and supplied energy. A strong effect of powder hollowness on the efficiency of MT has been known long ago: under identical mechanical loading of powder, the efficiency measured by instrumental tests (broadening of ESR lines, X-ray reflections) or by absorption methods (BET) drops for one order with compacting of a powder of ~40 to ~70% from theoretical density for MgO as an example [4].

In order to reveal the mechanism of chemical reactions, we used a standard approach – kinetic investigation or more precisely - study of the dynamics of mechanosynthesis versus the supplied mechanical energy, since the time of MT has no physical sense. An AGO-2 mill was used for mechanosynthesis of mixed oxides. The number of parameters which may affect the dynamics of mechanosynthesis was estimated to be ~20, so, in order to study the mechanism, we chose a model reaction $MeO+Me'O_3=MeMe'O_4$, presenting >20 systems with various physical and chemical properties. We chose the calculated effective temperature of the reaction zone T_z, achieved due to the mechanical energy supplied by an averaged shock, as a parameter of mechanical loading. Mechanochemical yield $K=(1/E_{½})$ in kg/MJ (where $E_{½}$ is the supplied energy for the transformation degree $\alpha=½$) was chosen as a parameter characterizing the chemical response. A *linear* dependence with the correlation coefficient of r=0,67 and a clear threshold effect were observed between mechanical loading T_z and chemical response K [2]. Introduction of a correction for the difference in Mohs's hardness of reagents $K^*= K\cdot\exp(\gamma\Delta M)$ improved correlation sharply to r=0,84. This allowed us to propose a general equation for mechanosynthesis in the first act:

$$A + B \overrightarrow{\leftarrow} (A_{1-\delta}B)^* \rightarrow A_{1-\delta}B^* \qquad (1)$$

where $(A_{1-\delta}B)^*$ is the transient *dynamic state (D)** at the contact between particles, which is formed by the roller mass transfer mechanism, Fig. 1, *A*- hard and *B* – soft reagent. The composition of the primary product $A_{1-\delta}B^*$ is always deficient in the hard reagent. In other words, a product has a high content of vacancies in the case of ordering into the AB structure («*» means origin from the dynamic state). Taking into account the contribution of enthalpy, relative heat conduction of the ($HgO+MoO_3$) system with close hardness of reagents

(ΔM=0,5) and deviations of the product composition from stoichiometry, we obtain the following equation for the first act of loading:

$$T^*_f = [T_z + \beta \alpha_z T_{ch} \exp(-\gamma \Delta M)] \frac{M}{M^\wedge}(1+k) + \beta \alpha_z T_{ch} \exp(-\gamma \Delta M) \qquad (2),$$

where α_z is the reaction degree, T_{ch}·exp(-γΔM) is heating of the zone due to the heat effect of reaction with a correction for deviation of the composition, correction for the deviation of molecular mass M of the product $k = \Delta M/(M_B - M_A)/M_{max}(M_A + M_B)$.

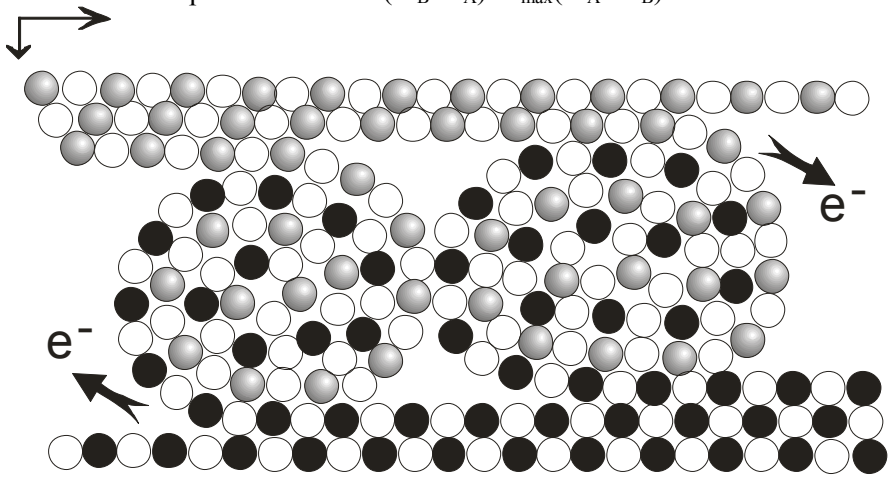

Fig. 1 Two-dimensional scheme for the formation of dynamic state *(D)** at the contact of particles during the primary act of loading.

Relative heat conductance is taken into account using a simple equation $M/M^\wedge$ ($M^\wedge$ is molecular mass of $HgO+MoO_3$), which replaces the modified Debye equation for the phonon contribution into heat conductivity $\lambda_{ph} \sim T_m^{3/2} \rho^{2/3}/M^{2/3} T$ for the systems used with the correlation coefficient r = 0,96. A linear correlation between T^*_f and K^* improves substantially up to r = 0, 9437, Fig. 2. In [2], with a more complicated equation (2), the value of r = 0,9414 was achieved. Taking into account semi-quantitative characteristics of Mohs's hardness and other approximations, the achieved a rather high r value. For instance, an evident dependence of MeO density ρ on molecular mass M is described by the linear correlation coefficient r = 0,96. The parameter γ = 0,144 reflects a decrease in mass transfer via roller (rotation) mechanism due to different hardness of reagents, as well as a reduction of enthalpy due to deviation from stoichiometry for the same reason. Parameter β has a simple physical sense: when any absorption of mechanical energy for grinding is absent, β = 1, since the enthalpy of the chemical reaction should have a double contribution with respect to mean heating of the zone by the supplied mechanical energy, because half of contacts of *A-A* and *B-B* types are chemically inactive but absorb mechanical energy. A maximum of the linear correlation $K^* \sim T^*_f$ is achieved for β = 10,2. In other words, only one tenth of theoretically possible mechanical energy is supplied to chemically active contacts; the remaining energy is consumed for grinding, mechanical activation (formation of structural defects) and aggregation of particles.

Comparison between the calculated data on relative heating in the first act of loading is made with experimentally determined yield obtained after tens of acts of loading. This forced extrapolation is quite correct in view of the similarity between kinetic curves and relative comparison of the systems, while the error thus introduced is one order smaller than the experimental error of $E_{½}$ determination.

Validity of equation (1) is confirmed independently by different methods. XRD

analysis of the crystalline products with scheelite structure $MeMe'O_4$ derived by mechanosynthesis at the degree of reaction $\alpha = 0,5 \div 0,9$ showed not only qualitative agreement with the theory, that is, deficit of the hard reagent in the crystal structure, but also a good quantitative correlation between deviation from stoichiometric composition and difference in hardness ΔM, $r = 0,91$ [5]. According to powder XRD structure analysis, high content of vacancies is observed for all mixed oxides derived by mechanosynthesis. For example, in the Aurivillius phase doped by different cations for stabilization of the γ-$Bi_2VO_{5.5}$ structure, the mean content of vacancies is about 20% [6]. The density of $BaTiO_3$ powder after MT, measured by helium pycnometry, is only 0,908 from the theoretical one [2], which coincides with the value expected on the basis of simple geometric considerations for the products with origin from *(D)**. An independent confirmation of high density of vacancies in $FeTiO_3$ (=loosening of the structure) as a result of MT was obtained as well in [7], where the authors observed decreasing of the Mossbauer effect in 2 times after 10 min and 2,5 times after 60 min of treatment in the same AGO-2 mill. In fact, γ–resonance spectroscopy is a selective method for the investigation of MT powders, similar to NMR and ESR, but this important circumstance is not taken into consideration [8-10].

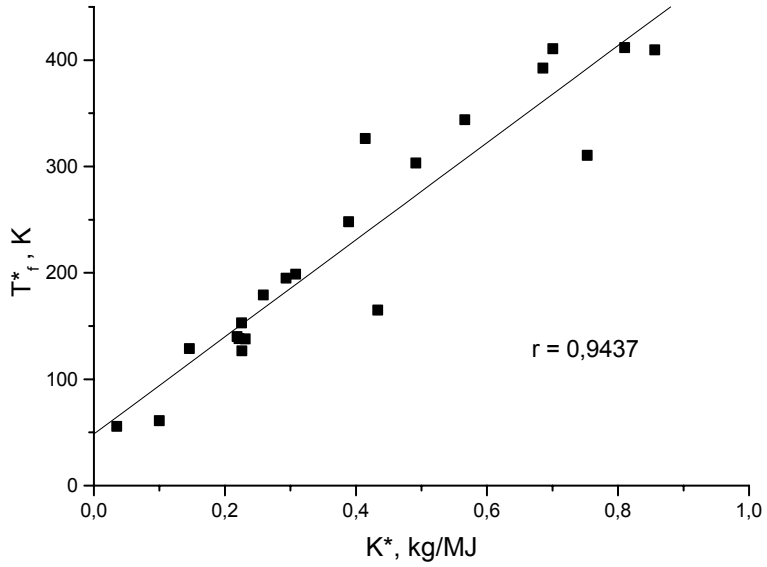

Fig. 2 Dependence of chemical response on mechanical loading in (MeO+$Me'O_3$) systems.

There are many reasons to assume that equation (1) is applicable for the case $A = B$, that is, for mechanical activation of individual compounds. In reality, mechanochemical reactions between oxides subjected to preliminary mechanical activation proceed in another route [2]:

$$PbO + WO_3 \rightarrow [Pb_2WO_5] \quad (3.1)$$

$$PbO + WO_3^* \rightarrow [PbWO_4] \quad (3.2)$$

$$CdO + PbO_2 \rightarrow [Cd_2PbO_4] \quad (4.1)$$

$$CdO + PbO_2^* \rightarrow [CdPbO_3] \quad (4.2)$$

where the structural type of the product is indicated in square brackets. Changes in the reaction route are equivalent to a decrease in Mohs's hardness for reagent *A**.

So, the main factors for the dynamics of mechanosynthesis are revealed by linearization of the dependence of response on loading: molecular mass of simple oxides (determining density, heat conductance and heat capacity), enthalpy of the chemical reaction

and the difference in the Mohs's hardness ΔM of reagents, which determines also the composition of the dynamic state *(D)** and the primary product. The threshold effect and linear dependence of the chemical response on effective temperature are the evidence of the leading role of the non-diffusion roller mechanism in mass transfer. The difference in hardness ΔM = 4 is a threshold for mechanosynthesis concerning the mechanical properties of reagents.

Theoretical estimations of interactions at the contacts between particles are possible only for the first loading act. The products of mechanosynthesis can really be observed by XRD after $10\text{-}10^2$ acts, that is, the section dealing with *secondary acts* is an important part of the theory. At the same time, these notions are absent in literature, though secondary acts are responsible for interesting phenomena – coalescence of crystallites during MT to 100 nm (!) [11-12] and the so-called *mechanochemical equilibrium* [13]. In [1-2], in order to accent the formation of *(D)**, primary and secondary acts of loading were assumed to be clearly distinguished from each other. Primary acts were characterized by a superfast roller mechanism of mass transfer with the formation of *(D)**, while secondary acts slowly approximated the composition of the product to the composition of the mixture in a deformation mixing regime by diffusion mass transfer. In reality, the same deformation mixing can also be represented as the formation of rotation zones with diffusion mass transfer during stoppage of rotations and unloading. Rotation fields are formed even in dense solids at strong plastic deformation, which leads to the loss of their integrity and to loosening [14]. It is natural to assume that the rotation (roller) contribution into mass transfer decreases gradually with an increase in the number of loadings, that is, modified equation (1) is also applicable for secondary processes:

$$A_xB^* + A_yB^* \rightarrow (D)^{*2} \rightarrow [A_nB_m] + B^* \text{ (or } A^*) \qquad (1.2)$$

Differences in the efficiency of mass transfer in primary and secondary acts within such an approach are due to lowering of the probability of overcoming the threshold because of a decrease of the enthalpy contribution into the formation of the dynamic state. Large differences in the efficiency of mass transfer via different mechanisms can be determined using different methods, including the approach dealing with the composition of crystal products of mechanosynthesis at different transformation degrees, which has been done several times [15]. In the case of substantial difference in compositions between starting mixture of oxides and *(D)**, and formation of a crystalline solid solution which is tolerant to deviations from stoichiometry, a typical dynamics of mechanosynthesis can be observed with the formation and disappearance of the primary product, Fig. 3.

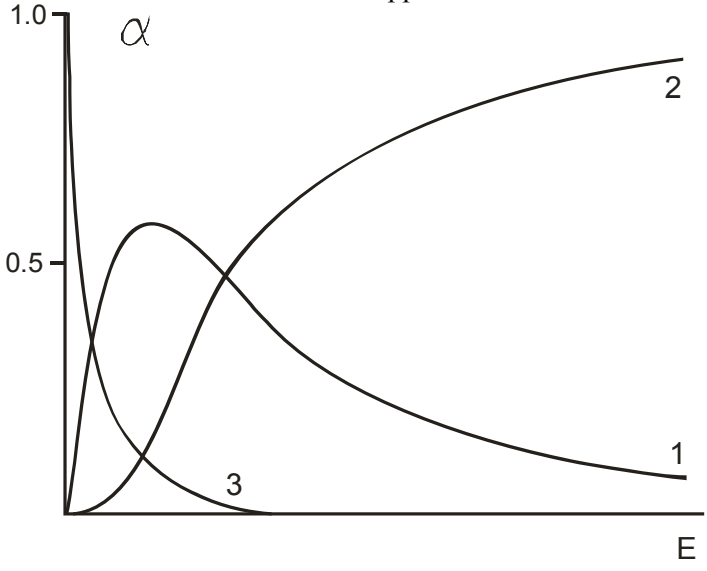

Fig. 3 Dynamics of mechanosynthesis in systems with the intermediate primary product according to XRD data: 1 – primary product, 2- secondary product, 3- initial reagents.

For primary products, $E_{½}$ is independent on the composition of the starting mixture. Quite the contrary, $E_{½}$ for secondary products is determined by the composition of the mixture. Mechanosynthesis rate distribution is shown in Fig. 4 for all investigated systems with the use of the correct MT procedure. The difference between the dynamics of the formation of primary and secondary products is about 1 order, which independently confirms the notions about substantially different contributions of non-diffusion (roller) and diffusion mechanisms into mass transfer in the primary and secondary acts.

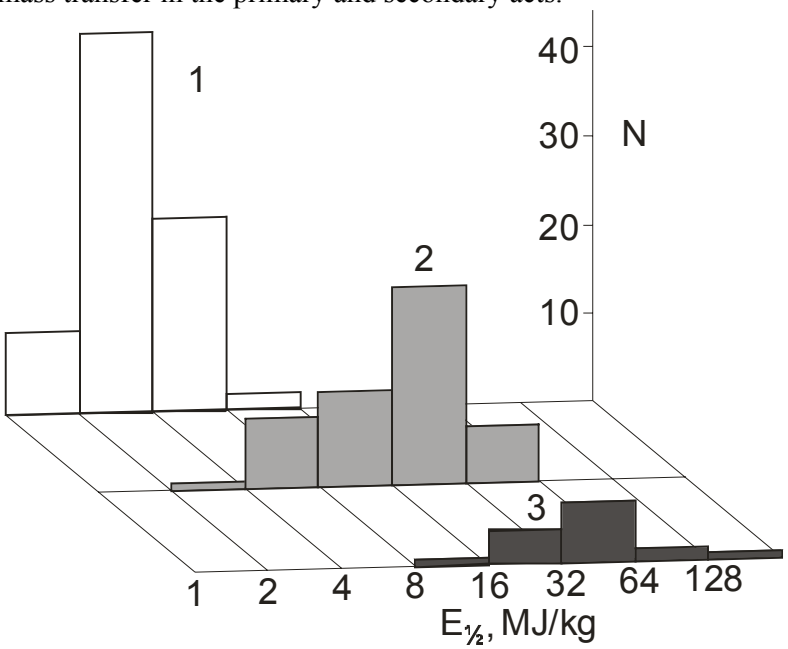

Fig. 4 Rate distribution for mechanosynthesis in studied oxide systems using the correct procedure. 1- primary, 2- secondary, 3- reduced products.

Secondary processes are transformations with the participation of the products of mechanosynthesis or reagents after loading (originating from *(D)**). Reactions of synthesis with activated reagents leading only to variations of the composition of primary product can be related to such processes:

$$A + B^* \rightarrow A_{1-\delta-x}B^* \quad (5.1)$$

$$A^* + B \rightarrow A_{1-\delta+x}B^* \quad (5.2),$$

but they are improbable when $\alpha<0,5$ because of zero enthalpy contribution into the threshold process of the formation of A^* and B^*. Secondary products are formed via reactions:

$$A + A_{1-\delta}B^* \rightarrow A_{2-\gamma}B^* \quad (5.3)$$

$$B + A_{1-\delta}B^* \rightarrow A_{1-\gamma}B_2^* \quad (5.4)$$

$$A^* + A_{1-\delta}B^* \rightarrow A_{2-\varepsilon}B^* \quad (5.5)$$

$$B^* + A_{1-\delta}B^* \rightarrow A_{1-\varepsilon}B_2^* \quad (5.6).$$

They become substantial when the primary product is accumulated. Coalescence of the primary product:

$$A_{1-\delta}B^* + A_{1-\delta}B^* \rightarrow [A_{1-\delta}B^*] \quad (5.7).$$

Coalescence of the secondary products:

$$A_{2-\gamma}B^* + A_{2-\gamma}B^* \rightarrow [A_{2-\gamma}B^*] \quad (5.8)$$

$$A_{1-\gamma}B_2^* + A_{1-\gamma}B_2^* \rightarrow [A_{1-\gamma}B_2^*] \quad (5.9)$$

$$A_{2-\varepsilon}B^* + A_{2-\varepsilon}B^* \rightarrow [A_{2-\varepsilon}B^*] \quad (5.10)$$

$$A_{1-\varepsilon}B_2^* + A_{1-\varepsilon}B_2^* \rightarrow [A_{1-\varepsilon}B_2^*] \quad (5.11).$$

Coalescence processes with a chemical interaction:

$$A_{2-\gamma}B^* + A_{2-\varepsilon}B^* \rightarrow [A_{2-\nu}B^*] \quad (5.12)$$

$$A_{1-\gamma}B^* + A_{1-\varepsilon}B^* \rightarrow [A_{1-\nu}B^*] \quad (5.13),$$

and so on (square brackets show here the growth of crystalline size). During loading, energy is introduced into a non-uniform chemical system; the energy promotes homogenisation at the atomic level; during unloading, its dissipation occurs, which can be accompanied either by continuation of homogenizing by means of diffusion, or by an inverse segregation process. The system after multiple cycling comes to some equilibrium, if we do not take into account slow change in composition due to reduction or post-reactions with the gas atmosphere. The direction of relaxation of the transient dynamic state *(D)** or *(D)*²* depends on its composition and size. If the size (thickness) *(D)** is smaller than some limit, the transient dynamic state may decompose on the surface of mother phases without forming the product. If the composition of the dynamic state is close to the composition of some structural type, relaxation proceeds in agreement with equation (11.3) into this ordered state, which can be observed by the XRD method. If no stable structural type exists for a given composition, a disordered (amorphous) energy-saturated state is formed. If the composition of the mixture is close to two structural types, *mechanochemical equilibrium* is established in secondary acts. In earler work mechanochemical equilibrium was sought for because of the unusual composition of the products. For example, MT of system ($2PbO+MoO_3$) resulted in a mixture of two phases with the structures [$PbMoO_4$] and [Pb_2MoO_5] [13]. In a neighbouring system with a similar phase diagram ($2PbO+WO_3$) the expected product with [Pb_2WO_5] structure appeared first together with [$PbWO_4$], but disappeared after a long time of MT [2]. The unusual phase composition of the products derived by mechanosynthesis in the case of mechanochemical equilibrium was explained in [2] by the formation of strongly non-stoichiometric compounds and by a competition between two structural types for the deficient reagent, in this case $M'O_3$. It should be noted that there is no principal difference between the processes with usual and unusual phase compositions of the mixture after MT. Both cases are described by one equation (1.2). The essence of tribochemical and mechanochemical equilibrium is caused by the competition between different structural types, remaining during a loading, for the disordered noncrystalline state during unloading. Ordering leads to the release of heat energy comparable with the energy of crystallization, which increases the time of relaxation and promotes the coalescence process.

Mechanosynthesis leads in a half of studied systems to other products than in the case of conventional solid phase reactions. A list of structural types observed for crystalline products derived by mechanosynthesis is very limited. For example, perovskites and fluorites were observed very often (~ 50%). The compounds with the following structural types have been obtained by mechanosynthesis: pyrochlor, scheelite, spinel, rock salt, bcc, sillenite, columbite, clinobisvanite, the simplest representatives of layered structures K_2NiF_4, Cd_2PbO_4, γ-$Bi_2VO_{5.5}$ and Bi_2GeO_5 (Aurivillius phases), and several structures represented for the present moment by one compound each. One can note that mechanosynthesis results in the formation of structures which easily form solid solutions. The mechanism of mechanosynthesis does not allow forming of stoichiometric compounds. Chemical inhomogeneity is very high even in single phase samples according to the XRD method [11]. One may say that statistical analysis of the structures derived by mechanosynthesis confirms independently the mechanism obtained by the analysis of dynamics.

Nano-structurization of mechanochemical powders

Investigation of the powders by means of structural and adsorption methods allows us to represent the nature of mechanochemical powders in a more complete manner. Separation of mechanochemical powders into fractions with the help of an electro-mass-classifier

technique (EMC) not only gives evidence of strong aggregation of powders and broad size distribution of the agglomerates but also provides the possibility of their practical application. Electron microscopic images of agglomerates, aggregates and crystallites are shown in Fig. 5.

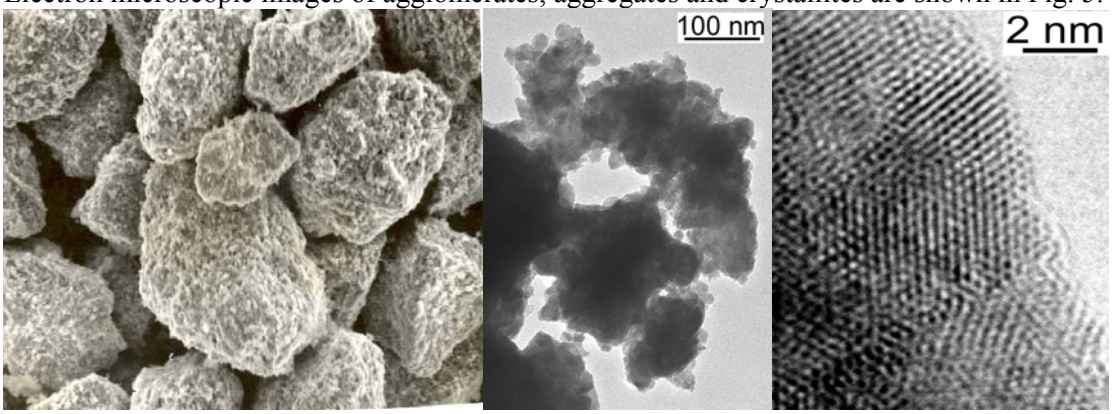

Fig. 5 EM image of the fraction of 40-100 μm agglomerates, aggregates and crystallites of fluorite $Bi_{1.5}Y_{0.3}Sm_{0.2}O_{3+x}$.

Agglomerates with a size up to 100 μm possess density of about 65-75% depending on size and the time of MT. They are composed of aggregates with the density up to 80 % and the size up to 1-2 μm. The aggregates are composites of nano-sized crystallites in an amorphous matrix, Fig. 5. For $BaTiO_3$ grinding, a mean crystallite size of 30 nm (specific surface area upon BET 33 m^2/g) was achieved after MT in M-3 for 9 min. In powders derived by mechanosynthesis the size of crystallites varied from ~5 to 100 nm according to estimations from broadened peaks using Sherrer's equation. During high energy ball milling, the density of crystallites decreases to ~90% of the theoretical value [2]; the density of mechanochemical products can be even lower. HREM image of ~20 nm crystallites displays nano-domains, small-angle boundaries and twins, Fig. 5.

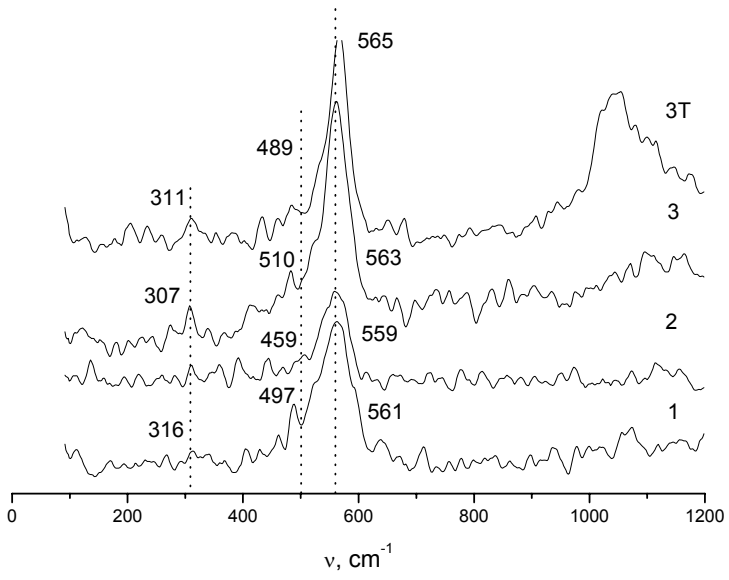

Fig. 6 Raman spectra of perovskites obtained by MT. 1- $(Ba_{0.5}Sr_{0.5})BiO_3$, 2- $BaBiO_3$, 3- $(Ba_{2/3}Bi_{1/3})BiO_3$, 3T- $(Ba_{2/3}Bi_{1/3})BiO_{8/3}$.

The existence of an atomic and electron domain structure is also confirmed by X-ray structural analysis and spectroscopic investigations. For example, $BaBiO_3$ possesses a

perovskite structure only in the limited range of compositions [16]. Metastable cubic perovskites $BaBiO_3$, $(Ba_{2/3}Bi_{1/3})BiO_3$, $(Ba_{0.5}Sr_{0.5})BiO_3$ were obtained by mechanical activation and mechanosynthesis. Bismuth atoms occupy both A and B positions in the perovskite ABO_3 structure. Such disordering of substitution was observed in a number of other structural types with two cation sublattices, for example in Aurivillius phases [6], in pyrochlores and in compounds with the Cd_2PbO_4 structure. However, short-range order often does not display high symmetry of perovskite structure with the Pm3m space group. Raman spectra of these samples are presented in Fig. 6, as well as $(Ba_{2/3}Bi_{1/3})BiO_{8/3}$ after heating to 420 ºC with loss of oxygen. Unlike for the equilibrium perovskite $BaBiO_{3-x}$ the Raman spectra contain an additional band (or a group of bands) near 500 cm^{-1}, while the band at 619 cm^{-1}, assigned to the pyramidal cluster with localized bipolaron [17], is absent. Differences between mechanochemical and usual powders are also exhibited in the IR spectra. The appearance of the band of carbonate ion absorption at 1100 cm^{-1} is the evidence of high reactivity of mechanochemical powders supersaturated with vacancies.

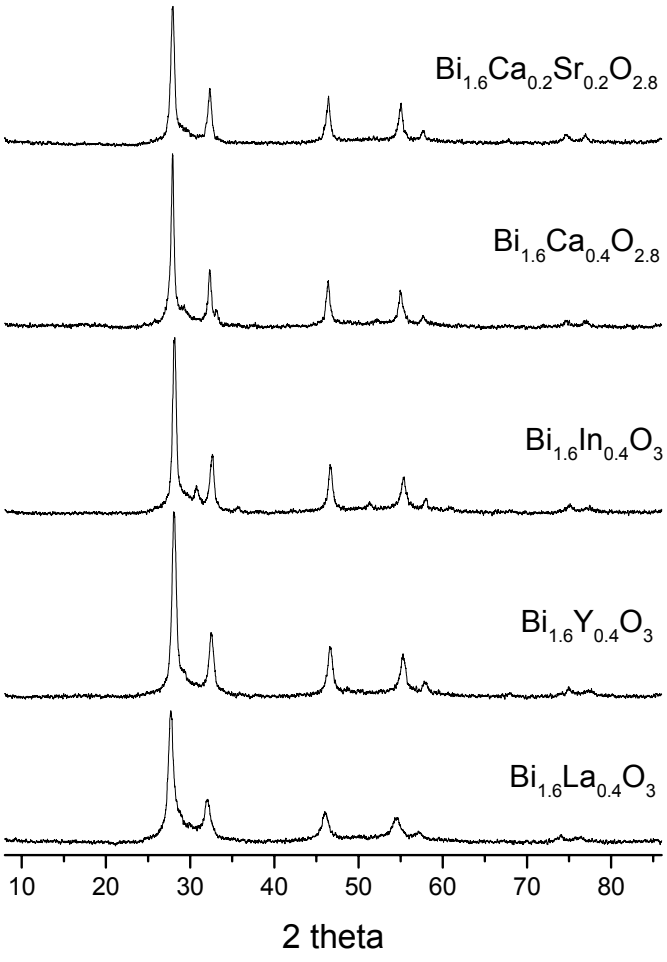

Fig. 7 X-Ray Diffraction patterns of fluorites (Cu K_α radiation) derived by mechanosynthesis.

Metastable fluorites were obtained by mechanosynthesis in the Sb_2O_3-CaO, Sb_2O_3-Bi_2O_3, $Bi_{1.6}M_{0.4}O_{3-x}$ systems (M= Ca, Sr, Y, In, La, Fig. 7). According to the powder XRD structural analysis, a shift of bismuth, yttrium and indium atoms along the [111] axis with a

lowering of local symmetry is observed in $Bi_{1.6}M_{0.4}O_{3-x}$ fluorites [18]. This disordering of the "anti-glass" type is a common characteristic of the compounds derived by mechanosynthesis. For example, the absence of short-range order in lead vanadates was established in [19] using a combination of ESR, NMR and XRD structural analysis. Very strong fluorescence in the Raman spectra was observed for all powders derived by mechanosynthesis. Drastic changes in the spectra were discovered after annealing. The Raman spectrum of $CaSb_4O_7$ disappears after annealing at ~490 ºC. With an increase in annealing temperature, Raman scattering appears again, but usual spectra with characteristic bands appear only after annealing at T~800 ºC [20]. Quite similar phenomenon was observed in other samples, including those with a perovskite structure. Fluorites in the Sb_2O_3-Bi_2O_3 system are black, changing colour into yellow after heating at ~500 ºC. At higher temperatures, structural transformations are observed by XRD. The conductance of black fluorite is low enough and corresponds to insulators. The obtained results can be explained by multi-level nano-structurization of disordered metastable compounds: formation of atomic and electron domains, clusters, multi nucleus complexes and Me-O radicals, correlation bags with non-localized itinerant electrons. Similar domains were observed in the $La_{2-x}Sr_xCuO_4$ family, which exhibit different properties: from polaron gas to superconductivity depending on composition and T [21].

Sintering

Sintering of the powders depends on many parameters. In order to determine the major factors, we carried out investigations on a model $BaTiO_3$system [22]. Powders with different particle size and granulometric composition were prepared from $BaTiO_3$ of different origin derived by the usual solid phase reaction and by decomposition of barium titanyloxalate (below referred to as d-$BaTiO_3$) by grinding for 9 min in a M-3 planetary mill and separation by the EMC technique. By choosing pressing conditions, we made disc samples identical in size and density (68-70%). These samples were sintered under the same conditions: rising up to sintering temperature 1300 °C for 1 h, 1 h exposure, and slow cooling with the furnace. The d-$BaTiO_3$ powders possessing poor compressibility were preliminarily treated in the same mill and separated in EMC in order to provide the same morphology and density of the compacted samples. We also studied for comparison radiation-thermal sintering of the pellets in electron beam (E = 1,4 MeV) at the same conditions, as well as preliminary treatment of the pellets in the beam at 110 °C, followed by thermal sintering. The results of sintering are shown in Fig. 8 as a dependence of residual porosity on the calculated particle size. Linear dependence was observed for the so-called uniform powders within the range of nearly two orders of particle size. Deviation from a linear dependence with increasing of porosity is due to the formation of large pores and cavities exceeding the size of initial particles, that is, due to non-uniformity of powders conserved in the pressed samples. The best ceramics with the density of 98,8±0,2 %, was obtained from a powder with a mean crystallite size of 30 nm and aggregate size < 1-2 μm. In the presence of agglomerates the density of sintered ceramics was lower than was expected from the linear dependence. The micro-structure of the ceramics reflects non-uniformity of the powders: for the powders from aggregates < 1-2 μm grain size is about 3-4 μm, while in the presence of agglomerates up to 100 μm the grain size was also within 1 – 100 micrometers. The obtained results confirm Balshin's law: zonal isolation of shrinkage during sintering of non-uniform powders. Non-uniformities less than 1 μm do not develop during sintering under the indicated conditions.

Other important factors were revealed by comparing sintering of $BaTiO_3$ samples of different origin. For the same morphology of powders, pressed d-$BaTiO_3$ pellets sintered much worse. During the solid phase synthesis of $BaTiO_3$ from $BaCO_3$ and TiO_2, crystal grains of the product keep topochemical memory about the reaction and the sources of Ba^{2+} and Ti^{4+}

in the form of the gradient of their vacancies concentrations. Sintering with shrinkage and rapprochement of the centres of particles is possible only in the case of volume diffusion, which is determined by the concentration of vacancies in the structure [23]. In the case of d-$BaTiO_3$ the concentration of vacancies is minimal and is determined by the Schottki mechanism of their formation. So, the concentration of vacancies in the structure determines sintering activity, other conditions being kept constant.

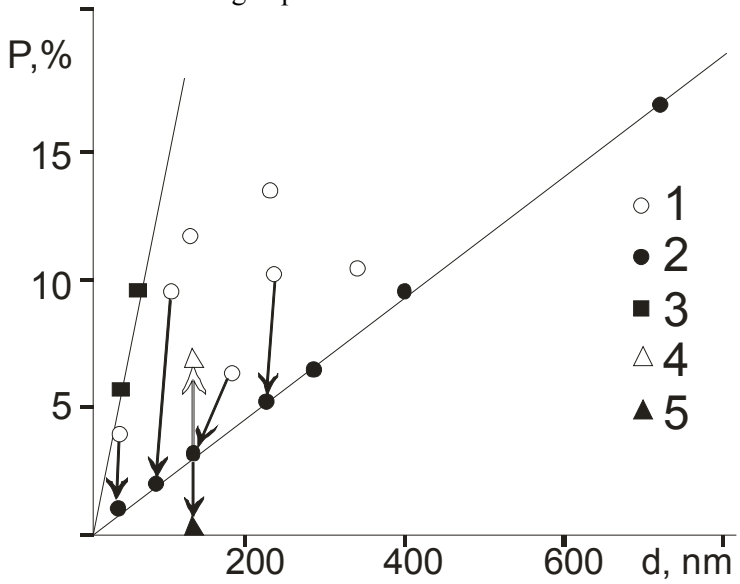

Fig. 8 Dependence of residual porosity of ceramics on the initial powder particle size after sintering at T=1300 ºC for 1 h. 1- $BaTiO_3$ after grinding in a planetary mill, 2- after additional treatment in EMC, 3- d-$BaTiO_3$ after treatment in a planetary mill and EMC, 4- preliminary treatment of the pressed powder 2 in an electron beam at 110 ºC, 5- sintering of pressed powder 2 in an electron beam at 1300 ºC.

Radiation thermal treatment of the pressed samples in an electron beam, carried out before thermal sintering, brings evidence to confirm this conclusion. Even at low temperature (110 °C) irreversible changes occur in $BaTiO_3$ samples: sintering activity decreases noticeably. This result can be explained by the formation of hot spots during relaxation of quasi-particles (plasmons, etc.), which arise when the hot electrons pass through a solid. Quasi-particles with the energy comparable with the energy of chemical bonds have an elevated probability of relaxation in the defective sites of the lattice, that is, at the grain boundaries and in the fields enriched by point defects. Local overheating of the lattice causes the annealing of vacancies, decrease in concentration gradient and lowering of the activity during subsequent sintering. The action of accelerated electrons, which is equivalent to homogenization of the composition at the atomic level of structure, was called electron mixer and confirmed afterwards by structural investigations of $YBa_2Cu_3O_{7-x}$ [24]. While approaching the eutectic point in the Y-Ba-Cu-O system, the radiation effect disappears. Radiation thermal treatment of d-$BaTiO_3$ samples under the same conditions does not cause noticeable changes in the properties, because the powder is chemically uniform. Radiation thermal sintering of the ceramics at the same conditions, in spite of the annealing of vacancies at the heating stage, provides obtaining of 99,9 % dense ceramics with a grain size 2-3 μm, that is, almost equal to the size of aggregates in the initial powder. In this case, local overheating of the grain boundaries provides maximally efficient rearrangements of particles and high density of ceramics with lowered rate of grain growth.

Investigation of sintering kinetics, as well as the studies of sintering of bimodal compositions comprising narrow fractions of crystal particles or isotropic agglomerates, microstructure and dielectric properties of ceramics allowed to establish different stages in the shrinkage process. At the stage of heating from 1200 to 1300 °C for 10 min the major part of shrinkage occurred: a decrease in porosity by 20-25%, while exposure at the maximal temperature 1300 °C provided a decrease 2% of porosity within 2 hours. During sintering of bimodal compositions, the density of ceramics and dielectric losses behave in a similar manner depending on the composition: smooth change in parameters only in the end compositions with small additives. However, the behaviour of permittivity was principally different. The composites of crystalline particles exhibited extremal dependence on composition, especially for the fractions with close particle sizes 6+8 μm, Fig. 9. Microstructure of the ceramics was unusual as well: isolated regions with high porosity from weakly contacting microcrystals with good faceting were surrounded by dense ceramics. This percolation microstructure of ceramics is responsible for the observed 4,5-fold increase in ε_{max} to reach 9000 (!) – nearly equal to that achieved after sintering of uniform nanopowders with the mean particle size 30 nm. These results provide unambiguous evidence for rearrangement of crystal particles as a whole at the initial step of sintering when the main shrinkage takes place. After that, rapprochement of particle centres occurs due to volume diffusion with the formation of good contacts between grains. The sintering process comes to an end by grain growth and coalescence of pores, which have almost no effect on shrinkage and bulk porosity [23, 25].

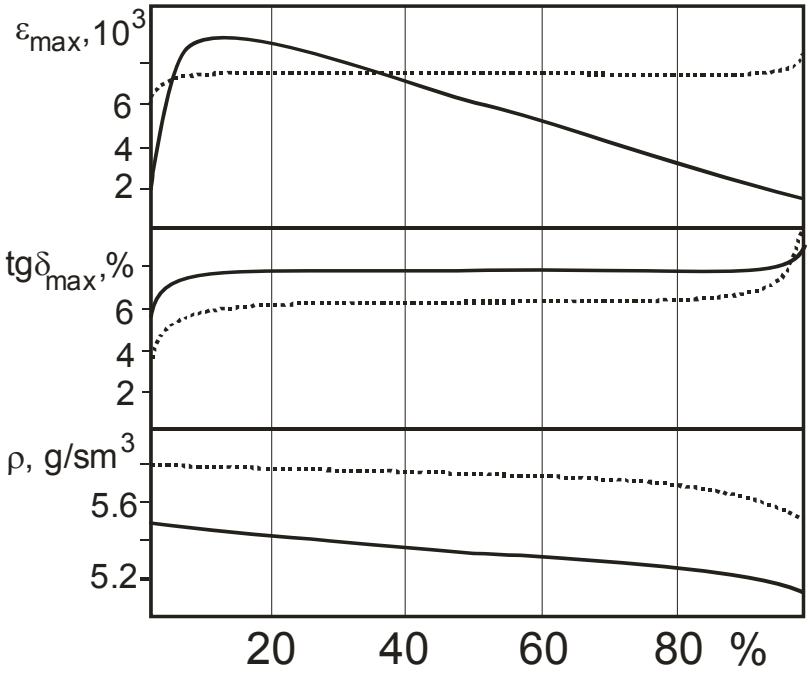

Fig. 9 Dependence of the parameters of $BaTiO_3$ ceramics on the composition of bimodal powders of crystalline particles 6+8 μm and agglomerates 3+21 μm (dotted lines).

It is impossible to investigate sintering of the powders of complex oxides derived by mechanosynthesis arranging experiments similarly to how it was done for barium titanate [22]. Single-phase mechanochemical powders are always nanocomposites of ordered (crystalline) grains in a disordered (amorphous or non-crystalline) matrix of another composition. One may assume *a priori* that reactive sintering complicated by structural transformations will take place during annealing these nanocomposites based on metastable

phases. An approximate sequence of processes is listed in Table I for two most typical cases: with partial decomposition of the metastable phase (sillenite Bi_2PbO_4 as an example), and without decomposition.

Tab. I. A sequence of processes during sintering of binary oxides derived by mechanosynthesis.

Process	**Bi_2PbO_4**		**Bi_2VO_5**	
	T, ºC	shrinkage	T, ºC	shrinkage
Defreezing of volume diffusion and growth of crystallites due to the amorphous state	250-400	+	250-400	+
Coalescence of crystallites till the aggregate size with the formation of grain, homogenisation of the grain composition and annealing of vacancies	350-480	++	350-550	++
Rearrangements of grains and coalescence with homogenisation of chemical composition	480-680 formation of the phase enriched by Pb	+++	550-880	+++
Changes in the oxidation degree	480-680 reduction of Bi^{3+}		550-880 partial oxidation of V^{4+} with decreasing of disordering (occupation of V positions by Bi)	
Melting point	680		880	

Sintering of Bi_2VO_5 in the air till rather dense ceramics (~95%) proceeds even at a relatively low temperature T= 727 ºC. The degree of structure disordering decreases only by a factor of 2 – total content of vacancies, related to partial occupation of vanadium positions by bismuth atoms, is conserved at a level of ~10% [6]. Oxygen conductivity of Bi_2VO_5 ceramics, doped by Sc, Sb, Zn, is closed to the highest value in BICUVOX [6]. This result, along with the formation of dense (90-95%) samples of $Bi_{0.8}M_{0.2}O_{2-x}$ nanocrystalline ceramics with fluorite structure, prepared by hot pressing as described in [18], demonstrates promising facilities of MCM to design new metastable ceramic materials.

Conclusion

The mechanism of superfast mechanosynthesis is established in the oxide systems. Under mechanical loading of the statistical ensemble of particles, the transient dynamic state is formed at the contacts of solids as a layer of growing rollers composed of the atomic mixture of reagents. The interaction product is formed during relaxation of the dynamic state under conditions of decompression and quenching. The major factors for the process dynamics are molecular mass of simple reagents, enthalpy of reaction and difference in the Mohs's hardness of reagents, which also determines the composition of the dynamic state and

primary product. Mechanosynthesis of mixed oxides is a threshold phenomenon with a linear dependence of the dynamics on effective temperature. The main contribution into mass transfer is brought with the non-diffusion (roller) mechanism. The diffusion contribution into mass transfer becomes noticeable in secondary acts. The reduction of oxides is caused by emission processes. Crystalline products of mechanosynthesis belong to a limited list of structural types which are stable to deviations from stoichiometry and inclined to form solid solutions.

Mechanochemical powders have clearly expressed multilevel structurization. Aggregates <1-2 μm and secondary agglomerates up to 100 μm are formed from nano-size particles. Particles are nanocomposites from relatively ordered crystallites in a disordered matrix. Crystallites are strongly disordered like "anti-glass" and consist of domains, twins. The morphology of powders which can be adjusted at the stages of MT and separation determines the microstructure of sintered ceramics and its properties. Supersaturation of structure by vacancies and chemical non-uniformity of mechanochemical powders promote sinterability at lowered temperatures, while high density of aggregates and reduced density of crystallites provide the high density of the green body after pressing and moulding. These features of the powders present the main advantages of the MCM with respect to other techniques of nano-powder preparation. Special outlooks of the MCM are related to obtaining unusual states of solids and new materials based on metastable phases, which cannot be achieved by other ways.

Acknowledgement

This work was supported by RFBR, Grants No. 95-03-080068, 99-03-32733, 02-03-33330, and INTAS, 01-2162.

References

1. V.V. Zyryanov. Inorg. Mater. 34, No. 12 (1998) 1525-1534 (in Russian).
2. V.V. Zyryanov. Mechanochemical phenomena in oxide systems. Thesis for Dr. Sci. in Chemistry, Novosibirsk. ISSC&M SB RAS. 2000 (in Russian).
3. V.V. Zyryanov, Sysoev V.F., Boldyrev V.V., Korosteleva T.V. USSR Inventor's Certificate No. 1375328. BI. No 7 (1988) 39 (in Russian).
4. V.V. Zyryanov, Isakova O.B. Izv. SO AN SSSR, ser. khim. Nauk, 3 (1988) 50-55 (in Russian).
5. V.V. Zyryanov. Inorg. Mater., 36, No. 1 (2000) 54-59.
6. V.V. Zyryanov, N.F. Uvarov. Inorg. Mater., 40 No 10 (2004) 1-7 (in Russian).
7. I.A.Maksutov, T.A.Pryakhina, A.A.Lysakov. Abstracts of XI All-Union Symposium on mechanochemistry and mechanoemission of solids, Chernigov. 1990. P.28-29 (in Russian).
8. N.V. Kosova, E.T. Devyatkina, E.G. Avvakumov et al. Inorg. Mater., 34, No. 4 (1998) 478-484 (in Russian).
9. Yu.T. Pavlyukhin, Ya.Ya. Medikov, V.V. Boldyrev. Doklady AN SSSR, 266 (1982) 1420-1423 (in Russian).
10. K.Tkachova, V.Shepelak, V.Boldyrev et al. J. Solid State Chem., 123 (1996) 100.
11. V.V. Zyryanov. Zhurn. Struktur. Khimii, 45, No. 3 (2004) 482-492 (in Russian).
12. B.B.Bokhonov, I.G.Konstanchuk, V.V.Boldyrev. Mat. Res. Bull. 30, No. 10 (1995) 1277.

13. V.V. Zyryanov. Izv. SO AN SSSR, ser. khim. Nauk, 2 (1990) 96-100 (in Russian).
14. Physical mesomechanics and computer design of materials. Ed. by Panin V.E. Novosibirsk, Nauka. 1995 (in Russian).
15. V.V. Zyryanov. Inorg. Mater., 35, No 9 (1999) 1101-1107 (in Russian).
16. J.K.Meen, O.A.Goksen, et al. Mat. Res. Soc. Symp. Proc., 658 (2001) GG9.14.1-6.
17. S.Kambe, I.Shime, S.Ohshima, K.Okuyama, K.Sakamoto. Solid State Ionics, 108 (1998) 307-313.
18. V.V. Zyryanov, N.F. Uvarov. Inorg. Mater., 40, No. 7 (2004) 729-734.
19. V.V. Zyryanov, O.B. Lapina. Inorg. Mater., 37, No. 3 (2001) 264-270.
20. V.V. Zyrianov. Proc. of Intern. Congress "Materiaux-2002". Tour, France. 2002. CM-01-007.
21. J.B. Goodenough. Mat. Res. Soc. Symp. Proc., 658 (2001) GG2.2.1-11.
22. V.V. Zyryanov, V.F.Sysoev, V.V.Boldyrev. Doklady AN SSSR, 300, No. 1 (1988) 162-165 (in Russian).
23. Ya.E. Geguzin. Physics of sintering, Nauka, Moscow, 1984, 312 p. (in Russian).
24. V.V. Zyryanov, S.E. Petrov, A.N. Kolyshev, A.P. Voronin. Izv. SO AN SSSR, ser. khim. nauk, 5 (1990) 130-134 (in Russian).
25. Processes of mass transfer during sintering. Ed. by Skorokhod V.V. Kiev, Naukova Dumka. 1987. 152 p. (in Russian).

Резюме: *Механизм реакций сверхбыстрого механохимического синтеза для оксидных систем предложен на основе исследования динамики процесса. Установлен пороговый эффект и линейная зависимость химического отклика от эффективной температуры в реакционной зоне. Определены главные факторы: молекулярная масса простых реагентов, энтальпия и разница реагентов в твердости по Моосу, которая влияет также на состав первичного продукта. Первичные акты характеризуются сверхбыстрым роликовым механизмом массопереноса с образованием переходного динамического состояния(D)*. Вторичные акты медленно приближают состав продукта к составу исходной смеси диффузионным массопереносом в режиме деформационного перемешивания с вкладом ротационного (роликового) механизма. Список структурных типов для сложных оксидов, полученных механосинтезом, включает перовскиты, флюорит, пирохлор, шеелит и ряд других структур. Порошки кристаллических продуктов демонстрируют многоуровневое структурирование. Во всех изученных сложных оксидах наблюдалось разупорядочение типа «антистекло». Механизм спекания был изучен на порошках $BaTiO_3$ различного происхождения и на метастабильных сложных оксидах, полученных механосинтезом. Главный вклад в усадку вносит подстройка кристаллических частиц как целого. Структурные превращения сопровождаются, как правило, спеканием неоднородных порошков, полученных механосинтезом.*

Ключевые слова*: механосинтез, нанопорошки, сложные оксиды, разупорядочение, спекание.*

Садржај: *Предложен је механизам за супер брзу реакцију механосинтезе за оксидне системе заснован на динамичкој студији. Утврђен је ефекат прага и линеарна зависност хемијског одзива од ефективне температуре у реакционој зони. Одређени су главни фактори: молекуларна маса реагенаса, енталпија и разлика реагенаса у тврдоћи по Мосу, која такође утиче на састав примарног продукта. Примарна дејства карактерише супербрзи котрљајући механизам транспорта масе са*

образовањем прелазног динамичког стања (D). Секундарним дејствима полако се приближава састав продукта и састав полазне смеше дифузионим преносом масе у режиму деформационог мешања уз дејство ротационог (котрљајућег) механизма. Листа структурних типова комплексних оксида добијених механосинтезом укључује перовските, флуорите, пирохлоре, шелите и низ других структура. Прахови кристалних производа имају вишеслојну структуру. У свим проученим комплексним оксидима уочена је јака неорганоизованост типа "анти-стакло". Механизам синтеровања проучен је на праховима $BaTiO_3$ различитог порекла и на метастабилним компексним оксидима који су добијени механосинтезом. По правилу, структурне трансформације су праћене синтеровањем нехомогених прахова добијених механосинтезом.*

Кључне речи: *Механосинтеза, нанопрахови, комплексни оксиди, неорганозованост, синтеровање, керамика.*